Table 5 – Validation of differentially expressed proteins by MRM assay. Differentially expressed proteins in the iTRAQ experiments were analyzed by MRM assay. The values represent the normalized area under the most intense peak of the target peptides, and are represented as mean ± SD. Duplicate analyses were performed for each of the mouse serum samples.

Accession number	Protein name	Peptide sequence	4-week-old				12-week-old			
			C57BL/6 (B6)	KK-A^y (A^y)	A^y/B6	*p*-Value	C57BL/6 (B6)	KK-A^y (A^y)	A^y/B6	*p*-Value
Q60994	Adiponectin	AVLFTYDQYQEK	1.62 ± 0.71	1.19 ± 0.40	0.74	0.28	1.55 ± 0.69	0.37 ± 0.08	0.24	0.01*
O89020	Afamin	AAPITQYLK	26.36 ± 12.46	22.51 ± 7.73	0.85	0.57	8.41 ± 2.1	9.67 ± 3.20	1.15	0.48
P11859	Angiotensinogen	TLHDQLVLAAEK	2.30 ± 1.01	1.78 ± 0.16	0.78	0.29	0.64 ± 0.27	0.85 ± 0.23	1.32	0.24
P32261	Antithrombin-III	TEDGFSLK	1.38 ± 0.54	0.18 ± 0.25	0.13	2.E−03*	0.62 ± 0.32	0.66 ± 0.32	1.08	0.81
Q00623	Apolipoprotein A-I	TQVQSVIDK	315.84 ± 67.55	0.10 ± 0.11	3.E−04	6.E−06*	84.87 ± 56.38	7.17 ± 5.33	0.08	0.02*
P09813	Apolipoprotein A-II	THEQLTPLVR	60.59 ± 24.63	171.35 ± 63.93	2.83	0.01*	8.07 ± 4.36	60.09 ± 26.56	7.45	3.E−03*
P08226	Apolipoprotein E	LQAEIFQAR	28.41 ± 13.60	37.81 ± 14.93	1.33	0.33	3.63 ± 1.1	15.66 ± 4.37	4.32	3.E−04*
Q01339	Beta-2-glycoprotein 1	YTSFEYPK	36.76 ± 12.77	24.30 ± 18.78	0.66	0.25	17.04 ± 4.23	23.48 ± 4.21	1.38	0.04*
Q8CIF4	Biotinidase	GLSSGLVTAALYGR	0.24 ± 0.06	0.23 ± 0.09	0.96	0.85	0.11 ± 0.08	0.11 ± 0.03	0.97	0.92
P23953	Carboxylesterase 1C	EGASEEETNLSK	10.65 ± 6.01	6.62 ± 5.93	0.62	0.32	1.09 ± 0.59	3.90 ± 4.75	3.57	0.23
Q9JJN5	Carboxypeptidase N catalytic chain	AVIQWIR	0.79 ± 0.27	1.20 ± 0.26	1.52	0.04*	0.39 ± 0.28	0.74 ± 0.16	1.92	0.04*
Q61147	Ceruloplasmin	AGLQAFFQVR	5.46 ± 4.68	12.49 ± 2.27	2.29	0.02*	1.19 ± 1.1	2.23 ± 1.36	1.87	0.22
Q06890	Clusterin	ASGIIDTLFQDR	2.48 ± 0.64	4.28 ± 0.79	1.57	0.02*	1.26 ± 0.38	2.58 ± 0.12	2.24	4.E−05*
Q8K182	Complement component C8 alpha chain	TEGTTVDEVQK	0.09 ± 0.04	0.05 ± 0.05	0.61	0.25	0.02 ± 0.02	0.06 ± 0.06	2.37	0.27
Q8BH35	Complement component C8 beta chain	ALEEFQSEVSSC[CAM]R	0.21 ± 0.10	0.99 ± 0.64	4.78	0.03*	0.08 ± 0.02	0.42 ± 0.65	5.32	0.28
P06683	Complement component C9	AVEDYIDEFSTK	0.13 ± 0.05	1.43 ± 0.67	11.07	3.E−03*	0.13 ± 0.15	0.19 ± 0.07	1.42	0.48
Q06770	Corticosteroid-binding globulin	AGEQINNHVK	0.08 ± 0.04	0.07 ± 0.05	0.91	0.82	0.10 ± 0.07	0.08 ± 0.05	0.80	0.59
Q91X72	Hemopexin	LYVSSGR	124.18 ± 37.50	98.01 ± 27.86	0.79	0.25	109.93 ± 37.67	126.32 ± 33.71	1.15	0.49
Q61704	Inter-alpha-trypsin inhibitor heavy chain H3	SLPEGVVDGIEVYSTK	0.21 ± 0.18	5.25 ± 2.72	25.18	3.E−03*	0.10 ± 0.05	0.30 ± 0.11	3.11	0.01*
O08677	Kininogen-1	QFNPGVK	11.81 ± 4.26	8.73 ± 3.31	0.74	0.24	8.84 ± 4.79	8.30 ± 3.43	0.94	0.84
P42703	Leukemia inhibitory factor receptor	ITGLVGPR	3.08 ± 0.87	8.78 ± 1.83	2.85	2.E−04*	2.7 ± 1.38	1.61 ± 0.37	0.60	0.12
P09581	Macrophage colony-stimulating factor 1 receptor	ESTSTGIWLK	1.02 ± 0.36	0.55 ± 0.25	0.54	0.04*	0.47 ± 0.24	0.35 ± 0.10	0.73	0.31
P04939	Major urinary protein 3	ENIIDLTNVNR	2.65 ± 0.65	2.89 ± 0.63	1.09	0.58	2.31 ± 1.1	1.52 ± 0.25	1.22	0.55
Q9ET66	Peptidase inhibitor 16	AESPEAEAESPLSSEALVPVLPAQER	0.03 ± 0.01	0.05 ± 0.01	2.10	4.E−03*	0.02 ± 0.01	0.01 ± 3E−03	0.56	0.07
P26262	Plasma kallikrein	SADNLVSGFSLK	1.09 ± 0.85	0.77 ± 0.47	0.71	0.49	0.09 ± 0.04	0.15 ± 0.08	1.66	0.15
P20918	Plasminogen	TGIGNGYR	0.16 ± 0.07	0.58 ± 0.34	3.69	0.03*	0.11 ± 0.06	0.18 ± 0.08	1.60	0.17
Q8R121	Protein Z-dependent protease inhibitor	LILVDYVLFK	0.17 ± 0.07	0.39 ± 0.18	2.33	0.04*	0.57 ± 0.28	0.54 ± 0.47	0.95	0.91
P19221	Prothrombin	DNLSPPLGQC[CAM]LTER	1.62 ± 1.41	2.21 ± 1.62	1.36	0.56	0.25 ± 0.14	1.04 ± 0.38	4.19	2.E−03*
P52480	Pyruvate kinase isozymes M1/M2	LDIDSAPITAR	0.11 ± 0.06	0.44 ± 0.31	4.19	0.04*	0.07 ± 0.04	0.06 ± 0.03	0.85	0.59
Q00724	Retinol-binding protein 4	LQNLDGTC[CAM]ADSYSFVFSR	0.39 ± 0.17	0.79 ± 0.20	2.01	0.01*	0.05 ± 0.03	0.11 ± 0.03	2.26	0.01*
P07759	Serine protease inhibitor A3K	TLFPSQIEELNLPK	0.39 ± 0.18	68.06 ± 28.55	176.70	7.E−04*	1.23 ± 2.06	9.28 ± 2.16	7.54	3.E−04*
P12246	Serum amyloid P-component	SQSLFSYSVK	0.13 ± 0.14	1.52 ± 0.44	11.59	2.E−04*	2E−03 ± 9E−04	0.21 ± 0.17	85.66	0.04*
Q8BND5	Sulfhydryl oxidase 1	SYVQFFFGC[CAM]R	0.30 ± 0.20	0.22 ± 0.14	0.73	0.48	0.07 ± 0.02	0.09 ± 0.03	1.19	0.42
P21614	Vitamin D-binding protein	TQVPEVFLSK	101.77 ± 35.17	88.03 ± 19.21	0.87	0.47	54.49 ± 21.66	70.01 ± 17.57	1.28	0.25

* $p < 0.05$ to age-matched C57BL/6 mice.

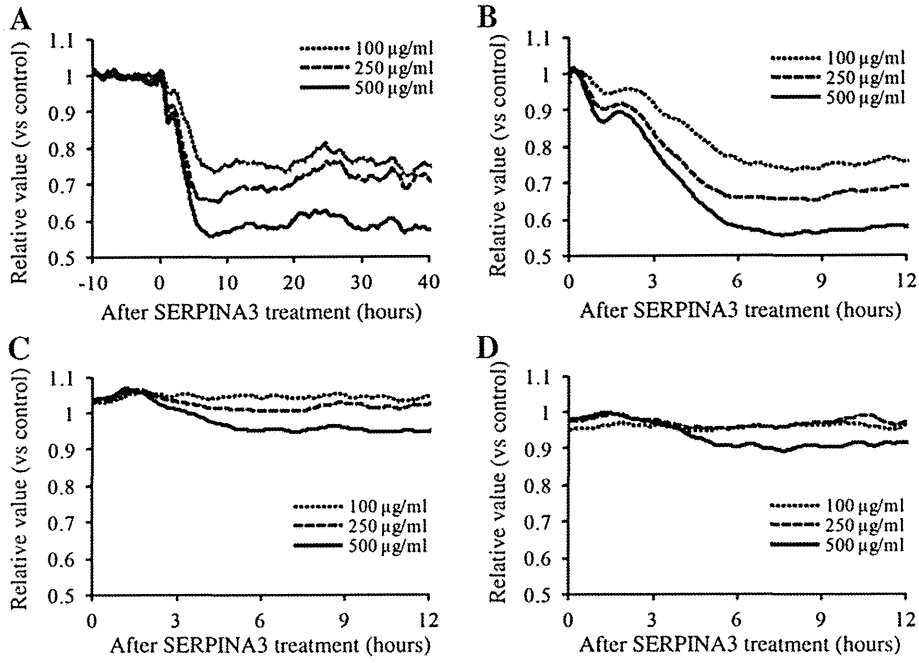

Fig. 4 – Monolayer barrier function of human retinal microvascular endothelial cells (HRMVECs) was notably decreased by SERPINA3 treatment. Post-confluent serum-starved HRMVECs were treated with SERPINA3 (100, 250, and 500 μg/ml) for 40 h. HRMVECs treated without SERPINA3 were used as control. (A) Impedance measurements at 16 kHz were obtained from HRMVECs treated with SERPINA3. (B–D) ECIS Zθ measurements were modeled to obtain the Rb (modeled barrier function, B), α (modeled cell-to-extracellular matrix interactions, C), and Cm (modeled membrane capacitance, D). Each trace of the impedance, Rb, α, and Cm is shown as an average of three replicate wells and representative of three independent experiments. Each value was normalized to the control.

in protein abundance among human serum obtained from a cohort of nondiabetic control subjects and patients diagnosed with T2DM [22]. The study reported here uses a similar approach nevertheless we analyzed the serum proteome analysis using T2DM mice model. However, it is novel in terms of quantitative profiling and comprehensive validation of the target proteins in individual samples. A limitation of this study is the use of T2DM mouse with obesity. We cannot delineate the differential markers of obesity and T2DM. Consequently, further validation analyses are required using human healthy and T2DM serum samples, which are now under investigation.

Among the eight serum proteins validated by MRM analysis, several published studies have also reported the differential expression of apo-AI, apo-AII, carboxypeptidase N catalytic chain, clusterin, inter-alpha-trypsin inhibitor heavy chain H3, SERPINA3K, and serum amyloid P-component in patients with diabetes and/or microvasculopathy [22–24]. Identification of RBP4 has not been reported in iTRAQ-based serum proteomic analysis, however, elevated levels of RBP4 have been reported in patients with obesity and metabolic syndrome [25–27]. The levels of RBP4 seem to be regulated in visceral adipose tissue. In the current study, SERPINA3K was chosen for further analyses because it remains to be elucidated whether human homologue, SERPINA3 is associated with the development of T2DM and/or diabetic retinopathy.

SERPINA3K was originally identified as a SERPIN family member with specific inhibitory effect on tissue kallikrein [28]. It is expressed in the liver, kidney, pancreas, and retina [29,30]. The previous studies have shown decreased retinal levels of SERPINA3K in a diabetic retinopathy rat model [19]. SERPINA3K attenuates inflammation in the retina with retinopathy [31] and has been found to inhibit ischemia-induced retinal neovascularization [20]. Recently, Zhang et al. have reported that rat SERPINA3K inhibited angiogenesis through Wnt/β-catenin signaling pathway as LRP6 antagonist [32]. In the present study, we found that SERPINA3K was consistently induced in KK-A^y mice sera compared with C57BL/6 mice. We also investigated the potential association between human SERPINA3 levels and T2DM. The serum SERPINA3 levels were approximately 180 μg/mL in healthy subjects, and the serum SERPINA3 levels were higher in T2DM and diabetic retinopathy patients compared to those in healthy control subjects (data not shown). In the IPA network analysis, SERPINA3 is shown to be modulated directly by Nfe2l2 (Fig. 2) [33]. Nfe2l2, also known as nuclear factor E2-related factor 2 (Nrf2) is a transcription factor that functions as a master regulator of the cellular adaptive response to oxidative stress [34]. Hyperglycemia is the metabolic hallmark of diabetes and leads to widespread cellular damage through oxidative stress. Recently, Slitt et al. reported that enhanced Nrf2 activation inhibited lipid accumulation in white adipose tissue, suppressed adipogenesis, induced insulin resistance and glucose intolerance, and increased hepatic steatosis in diabetic $Lep^{ob/ob}$ mice [35]. We analyzed the tissue distribution of SERPINA3 in KK-A^y mice and found that SERPINA3 is highly expressed in liver and also detected in pancreas, white adipose tissue, skeletal muscle, kidney, and heart (data not shown). We

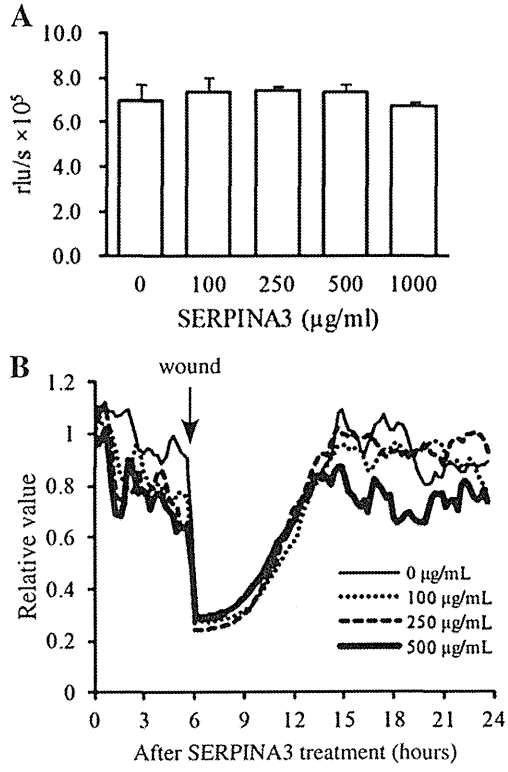

Fig. 5 – SERPINA3 did not significantly affect the proliferative ability or migratory capability of HRMVECs. (A) BrdU incorporation in HRMVECs. The cells were treated with or without SERPINA3 (100, 250, 500, 1000 μg/mL) and labeled with BrdU from 18 to 24 h after treatment. Data are expressed as mean ± SD values of triplicate samples. (B) Electrical wound-healing assay by ECIS Zθ. Post-confluent serum-starved HRMVECs were treated with SERPINA3 for 6 h, after which an elevated voltage pulse was applied to the electrode (marked with an arrow). Impedance values were normalized by dividing the values by those measured just prior to the addition of SERPINA3 (at time = 0).

speculate that enhanced activation of Nrf2 in liver may cause the increase in serum SERPINA3 from the early onset of T2DM although further studies are required to identify the precise mechanisms.

To gain insights into the function of SERPINA3, we assessed the effects of SERPINA3 on endothelial cell monolayer permeability. An ECIS assay was carried out by varying SERPINA3 concentrations ranging from 100 to 500 μg/mL, which cover the physiological concentration range in healthy subjects and T2DM patients. An *in vitro* assay revealed that SERPINA3 increased transendothelial permeability of HRMVECs (Fig. 5). Diabetic maculopathy, a leading cause of vision loss in patients with T2DM is characterized by hyperpermeability of retinal blood vessels with subsequent formation of macular edema and hard exudates. Epidemiological studies have suggested that glycemic control plays a major role in the development of vascular complications of diabetes [36]. SERPINA3 may become a downstream glycemic target that contributes to increased retinal vascular permeability that could be targeted therapeutically, and a blood biomarker of diabetic retinopathy although further investigations are required. In addition, our present study showed that SERPINA3 showed little proliferative ability and little effect of migratory capability of HRMVECs, which is inconsistent with the previous reports [20,32]. The discrepancy may have risen from interspecies differences. Rat SERPINA3K shares high degree of sequence identity with mouse SERPINA3K (70–71%) and human SERPINA3 (50–55%). However, mouse SERPINA3K and human SERPINA3 are known to be induced by acute inflammation in contrast to rat SERPINA3K which is a negative acute-phase protein [37]. Further studies are necessary to clarify the precise mechanism of action of SERPINA3 for cell proliferation.

In the current study, 11 of 45 differentially expressed proteins could not be validated by MRM analysis using an independent sample set. In MRM, there are several possible reasons why not all targeted proteins were detected. They include 1) the absence of appropriate peptide regions of the targeted proteins which meet the criteria described in the Materials and methods, and 2) the MS peak of the target protein was hard to be detected due to high background noise. For the validation of the 11 candidate proteins, we need to analyze the serum levels by other methods such as ELISA or Western blotting. We now investigate the potential association between the levels of the 11 candidate proteins and T2DM using human healthy and T2DM serum samples. We would examine the functional properties of the validated proteins including the 7 MRM-validated proteins in the future studies.

In summary, iTRAQ and MRM based discovery-through-verification strategy led to the identification of several differentially protein including SERPINA3K in T2DM. With the identified expressed proteins, our proteomics study could provide valuable clues to better understand the underlying mechanisms associated with T2DM.

Supplementary data to this article can be found online at http://dx.doi.org/10.1016/j.jprot.2013.03.014.

Conflict of interest

The authors report no conflict of interest.

Acknowledgments

We thank W. Iwata, T. Okamura, M. Goto and the technical staff of the Division of Animal Models at the National Center for Global Health and Medicine for their technical assistances. This work was supported by a Grant-in-Aid (Research on Biological Markers for New Drug Development, H20-009) from the Ministry of Health, Labor, and Welfare of Japan, a Grant-in-Aid for Scientific Research (KAKENHI, 23500870) from the Ministry of Education, Culture, Sports, Science and Technology of Japan, and a grant from the National Center for Global Health and Medicine (23S104).

REFERENCES

[1] Korc M. Diabetes mellitus in the era of proteomics. Mol Cell Proteomics 2003;2:399–404.

[2] Gerich JE. The genetic basis of type 2 diabetes mellitus: impaired insulin secretion versus impaired insulin sensitivity. Endocr Rev 1998;19:491–503.
[3] Klein R, Klein BEK, Moss SE, Cruickshanks KJ. The Wisconsin epidemiologic study of diabetic retinopathy: XVII. The 14-year incidence and progression of diabetic retinopathy and associated risk factors in type 1 diabetes. Ophthalmology 1998;105:1801–15.
[4] Horikawa Y, Yamasaki T, Nakajima H, Shingu R, Yoshiuchi I, Miyagawa J, et al. Identification of a novel variant in the phosphoenolpyruvate carboxykinase gene promoter in Japanese patients with type 2 diabetes. Horm Metab Res 2003;35:308–12.
[5] Vendrell J, Fernandez-Real JM, Gutierrez C, Zamora A, Simon I, Bardaji A, et al. A polymorphism in the promoter of the tumor necrosis factor-α gene (-308) is associated with coronary heart disease in type 2 diabetic patients. Atherosclerosis 2003;167:257–64.
[6] Lindgren CM, Widen E, Tuomi T, Li H, Almgren P, Kanninen T, et al. Contribution of known and unknown susceptibility genes to early-onset diabetes in Scandinavia: evidence for heterogeneity. Diabetes 2002;51:1609–17.
[7] Rao AA, Sridhar GR, Das UN. Elevated butyrylcholinesterase and acetylcholinesterase may predict the development of type 2 diabetes mellitus and Alzheimer's disease. Med Hypotheses 2007;69:1272–6.
[8] Rao AA, Sridhar GR, Srinivas B, Das UN. Bioinformatics analysis of functional protein sequences reveals a role for brain-derived neurotrophic factor in obesity and type 2 diabetes mellitus. Med Hypotheses 2008;70:424–9.
[9] On YK, Park HK, Hyon MS, Jeon ES. Serum resistin as a biological marker for coronary artery disease and restenosis in type 2 diabetic patients. Circ J 2007;71:868–73.
[10] Zhang R, Barker L, Pinchev D, Marshall J, Rasamoelisolo M, Smith C, et al. Mining biomarkers in human sera using proteomic tools. Proteomics 2004;4:244–56.
[11] Dayal B, Ertel NH. ProteinChip technology: a new and facile method for the identification and measurement of high-density lipoproteins apoA-I and apoA-II and their glycosylated products in patients with diabetes and cardiovascular disease. J Proteome Res 2002;1:375–80.
[12] Sundsten T, Eberhardson M, Goransson M, Bergsten P. The use of proteomics in identifying differentially expressed serum proteins in humans with type 2 diabetes. Proteome Sci 2006;4:22.
[13] Suto J, Matsuura S, Imamura K, Yamanaka H, Sekikawa K. Genetics of obesity in KK mouse and effects of A^y allele on quantitative regulation. Mamm Genome 1998;9:506–10.
[14] Unoki-Kubota H, Yamagishi S, Takeuchi M, Bujo H, Saito Y. Pyridoxamine, an inhibitor of advanced glycation end product (AGE) formation ameliorates insulin resistance in obese, type 2 diabetic mice. Protein Pept Lett 2010;17:1177–81.
[15] Huang da W, Sherman BT, Lempicki RA. Systematic and integrative analysis of large gene lists using DAVID bioinformatics resources. Nat Protoc 2009;4:44–57.
[16] Okumura A, Ohta H, Inoue Y, Enami I. Identification of functional domains of the extrinsic 12 kDa protein in red algal PSII by limited proteolysis and directed mutagenesis. Plant Cell Physiol 2001;42:1331–7.
[17] Giaever I, Keese CR. Micromotion of mammalian cells measured electrically. Proc Natl Acad Sci U S A 1991;88:7896–900.
[18] Nishimura M. Breeding of mice strains for diabetes mellitus. Exp Anim 1969;18:147–57.
[19] Hatcher HC, Ma JX, Chao J, Chao L, Ottlecz A. Kallikrein-binding protein levels are reduced in the retinas of streptozotocin-induced diabetic rats. Invest Ophthalmol Vis Sci 1997;38:658–64.
[20] Gao G, Shao C, Zhang SX, Dudley A, Fant J, Ma J-X. Kallikrein-binding protein inhibits retinal neovascularization and decreases vascular leakage. Diabetologia 2003;46:689–98.
[21] Klein R, Klein BEK, Moss SE, Cruickshanks KJ. The Wisconsin epidemiologic study of diabetic retinopathy. Opthalmology 1995;102:7–16.
[22] Kaur P, Rizk NM, Ibrahim S, Younes N, Uppal A, Dennis K, et al. iTRAQ-based quantitative protein expression profiling and MRM verification of markers in type 2 diabetes. J Proteome Res 2012;11:5527–39.
[23] Overgaard AJ, Thingholm TE, Larsen MR, Tarnow L, Rossing P, McGuire JN, et al. Quantitative iTRAQ-based proteomic identification of candidate biomarkers for diabetic nephropathy in plasma of type 1 diabetic patients. Clin Proteomics 2010;6:105–14.
[24] García-Ramírez M, Canals F, Hernández C, Colomé N, Ferrer C, Carrasco E, et al. Proteomic analysis of human vitreous fluid by fluorescence based difference gel electrophoresis (DIGE): a new strategy for identifying potential candidates in the pathogenesis of proliferative diabetic retinopathy. Diabetologia 2007;50:1294–303.
[25] Klöting N, Graham TE, Berndt J, Kralisch S, Kovacs P, Wason CJ, et al. Serum retinol-binding protein is more highly expressed in visceral than in subcutaneous adipose tissue and is a marker of intra-abdominal fat mass. Cell Metab 2007;6:79–87.
[26] Fernández-Real JM, Moreno JM, Ricart W. Circulating retinol-binding protein-4 concentration might reflect insulin resistance-associated iron overload. Diabetes 2008;57:1918–25.
[27] Raila J, Henze A, Spranger J, Möhlig M, Pfeiffer AF, Schweigert FJ. Microalbuminuria is a major determinant of elevated plasma retinol-binding protein 4 in type 2 diabetic patients. Kidney Int 2007;72:505–11.
[28] Chao J, Chai KX, Chen LM, Xiong W, Chao S, Woodley-Miller C, et al. Tissue kallikrein-binding protein is a SERPIN. I. Purification, characterization, and distribution in normotensive and spontaneously hypertensive rats. J Biol Chem 1990;265:16394–401.
[29] Chao J, Tillman DM, Wang MY, Margolius HS, Chao L. Identification of a new tissue-kallikrein-binding protein. Biochem J 1986;239:325–31.
[30] Gettins PG. SERPIN structure, mechanism, and function. Chem Rev 2002;102:4751–803.
[31] Zhang B, Hu Y, Ma JX. Anti-inflammatory and antioxidant effects of SERPINA3K in the retina. Invest Ophthalmol Vis Sci 2009;50:3943–52.
[32] Zhang B, Abreu JG, Zhou K, Chen Y, Hu Y, Zhou T, et al. Blocking the Wnt pathway, a unifying mechanism for an angiogenic inhibitor in the serine proteinase inhibitor family. Proc Natl Acad Sci U S A 2010;107:6900–5.
[33] Kwak MK, Wakabayashi N, Itoh K, Motohashi H, Yamamoto M, Kensler TW. Modulation of gene expression by cancer chemopreventive dithiolethiones through the Keap1-Nrf2 pathway: identification of novel gene clusters for cell survival. J Biol Chem 2003;278:8135–45.
[34] Ishii T, Itoh K, Ruiz E, Leake DS, Unoki H, Yamamoto M, et al. Role of Nrf2 in the regulation of CD36 and stress protein expression in murine macrophages: activation by oxidatively modified LDL and 4-hydroxynonenal. Circ Res 2004;94:609–16.
[35] Xu J, Kulkarni SR, Donepudi AC, More VR, Slitt AL. Enhanced Nrf2 activity worsens insulin resistance, impairs lipid accumulation in adipose tissue, and increases hepatic steatosis in leptin-deficient mice. Diabetes 2012;61:3208–18.
[36] American Diabetes Association. Implications of the diabetes control and complications trial. American Diabetes Association. Diabetes 1993;42:1555–8.
[37] Ohkubo K, Ogata S, Misumi Y, Takami N, Ikehara Y. Molecular cloning and characterization of rat contrapsin-like protease inhibitor and related proteins. J Biochem 1991;109:243–50.

FEBS Letters 587 (2013) 404–409

FEBS Letters

journal homepage: www.FEBSLetters.org

Leukocyte cell-derived chemotaxin 2 is a zinc-binding protein

Akinori Okumura [a,1], Takehiro Suzuki [b], Hideyuki Miyatake [b], Tomoya Okabe [c], Yuki Hashimoto [c], Takuya Miyakawa [d], Hai Zheng [d], Hiroyuki Unoki-Kubota [a], Hideaki Ohno [c], Naoshi Dohmae [b], Yasushi Kaburagi [a], Yoshitsugu Miyazaki [c], Masaru Tanokura [d], Satoshi Yamagoe [c,*,1]

[a] Department of Diabetic Complications, Diabetes Research Center, Research Institute, National Center for Global Health and Medicine, Tokyo 162-8655, Japan
[b] Biomolecular Characterization Team, RIKEN, Saitama 351-0198, Japan
[c] Department of Chemotherapy and Mycosis, National Institute of Infectious Diseases, Tokyo 162-8640, Japan
[d] Department of Applied Biological Chemistry, Graduate School of Agricultural and Life Sciences, The University of Tokyo, Tokyo 113-8657, Japan

ARTICLE INFO

Article history:
Received 5 September 2012
Revised 8 December 2012
Accepted 9 January 2013
Available online 22 January 2013

Edited by Christian Griesinger

Keywords:
Leukocyte cell-derived chemotaxin 2
Zinc-binding protein
Electrospray ionization mass spectrometry
X-ray absorption fine structure
Disulfide bond
Oligomerization

ABSTRACT

Leukocyte cell-derived chemotaxin 2 (LECT2) is a secreted hepatic protein that has been associated with several physiological activities. LECT2 belongs to the peptidase M23 family, suggesting that it is a zinc-binding protein. To test this possibility, electrospray ionization mass spectrometry and X-ray absorption fine-structure analysis were performed. Results of these experiments indicated that recombinant mouse LECT2 produced by an animal cell line contains a zinc atom. Furthermore, the recombinant LECT2 was found to be self-oligomerized by disulfide bonds in vitro, but this was suppressed by addition of zinc. These results indicated that zinc stabilizes the LECT2 structure.

Structured summary of protein interactions:
LECT2 and **LECT2** bind by cross-linking study (View interaction)
LECT2 and **LECT2** bind by comigration in gel electrophoresis (View interaction)
LECT2 and **LECT2** bind by comigration in gel electrophoresis (View interaction: 1, 2, 3)
LECT2 and **LECT2** bind by cross-linking study (View interaction: 1, 2, 3)
LECT2 and **LECT2** bind by comigration in gel electrophoresis (View interaction: 1, 2, 3)

1. Introduction

Leukocyte cell-derived chemotaxin 2 (LECT2) has been identified as a human neutrophil chemotactic protein [1]. LECT2 is a secreted hepatic protein with a molecular mass of approximately 16 kDa [2], and the mammalian form has three disulfide bonds [3]. The protein-sequence has been well conserved throughout evolution. Although accumulating evidence indicates that LECT2 is associated with several physiologic functions, their mechanisms are not yet clear [4–9].

LECT2 belongs to the peptidase M23 structural family (PF01551), as described in the pfam data base (http://pfam.sanger.ac.uk), which indicates it is a metalloprotease having a zinc ion as a cofactor. Actually, many proteins of the M23 family have a zinc ion in their catalytic domain that contributes to their protease activity. This protein family is widespread in bacteria, but LECT2 is the only vertebrate protein in the M23 family. It is unclear whether LECT2 has a protease activity.

In this report, the results of electrospray ionization mass spectrometry (ESI-MS) and X-ray absorption fine-structure (XAFS) analysis indicate that recombinant mouse LECT2 produced by a mammalian cell line contains a zinc atom. Furthermore, human and mouse recombinant LECT2 proteins produced by an animal cell line were found to be oligomerized by disulfide linkages in vitro. This oligomerization was accelerated by the presence of EDTA or EGTA and was inhibited by the presence of zinc ions. These results indicate that LECT2 is a zinc-binding protein and that zinc contributes to the stability of the protein structure. They also suggest that zinc plays a crucial role in the biological function of LECT2. Moreover, LECT2 has recently been reported as an amyloid protein [10,11], suggesting that the oligomerization of LECT2 observed in this study might be related to amyloid fibril formation.

2. Materials and methods

2.1. The purification of recombinant mouse LECT2 protein

Recombinant mouse LECT2 (GenBank accession number: BAA33383) was purified using a procedure slightly modified from the original [3]. A stable clone (clone No. 10G) of Chinese hamster

Abbreviation: LECT2, leukocyte cell-derived chemotaxin 2

* Corresponding author. Fax: +81 3 5285 1150.
E-mail address: syamagoe@nih.go.jp (S. Yamagoe).

[1] *These authors contributed equally to this work.*

0014-5793/$36.00 © 2013 Federation of European Biochemical Societies. Published by Elsevier B.V. All rights reserved.
http://dx.doi.org/10.1016/j.febslet.2013.01.025

ovary (CHO) cells transfected with an expression vector having mouse LECT2 cDNA was grown in Dulbecco's modified Eagle's medium with 5% fetal bovine serum. Five liters of culture medium were harvested and diluted with an equal volume of Milli-Q water. CM-Sepharose fast flow resin (GE Healthcare, Little Chalfont, UK), pre-equilibrated with 50 mM Tris–HCl pH 7.5 (buffer A), was added to the culture fluid (30 ml resin) and stirred for 16 h at 4 °C. The resin was collected by filtration with aspiration over a Kiriyama-rohto (95 mm in diameter, filter paper No. 5B; Kiriyama, Tokyo, Japan), washed exhaustively with buffer A, and eluted with buffer A supplemented with 0.5 M NaCl. The eluent was dialyzed against buffer A overnight, and then loaded onto a Toyopearl DEAE-650 M column (Tosoh, Tokyo, Japan) equilibrated with buffer A. The pass-through fraction was recovered and applied again to the Toyopearl CM-650 M column (Tosoh, Tokyo, Japan) equilibrated with buffer A. After the CM column was washed with buffer A, the proteins were eluted with a 0–0.7 M NaCl linear gradient in buffer A. LECT2-containing fractions were identified using an ELISA [5]. The fractions containing an appreciable amount of mouse LECT2 were pooled and dialyzed against 50 mM Tris–HCl pH 7.5 containing 10% glycerol (buffer B). The dialysate was loaded onto a Mono-S HR 5/5 column (GE Healthcare, Little Chalfont, UK) equilibrated with buffer B and washed with buffer B containing 0.1 M NaCl. Elution was then carried out with a linear gradient of 0.1–0.5 M NaCl in buffer B. The fractions showing a single band on SDS–PAGE by silver staining were pooled and dialyzed against 40 mM HEPES-NaOH pH 7.4, 10% glycerol, 100 mM NaCl. Recombinant human LECT2 was also purified from the culture fluid of an established CHO cell line (clone name C1D8) as described previously [3,12].

2.2. Electrospray ionization mass spectrometry (ESI-MS)

ESI-MS experiments were performed on a Thermo Finnigan LCQ Deca XP plus ion trap mass spectrometer (Thermo Scientific, Waltham, MA, USA) equipped with a handmade nanospray tip (0.1 × 50 mm). For the measurements under acidic and neutral conditions, the ESI-MS spectra were acquired in positive ion mode at a flow rate of 1 μl/min with running solution consisting of 0.075% formic acid (pH 2.6) and 10 mM ammonium formate (pH 6.4), respectively. Recombinant mouse LECT2 was exchanged into the same solution. Electrospray mass spectra were processed using the Biomass convolution and deconvolution algorithms in the Bioworks 3.1 software package (Thermo Scientific).

2.3. X-ray absorption fine structure (XAFS)

Recombinant mouse LECT2 and a recombinant lysostaphin of *Staphylococcus simulans* (Wako, Osaka, Japan) were dialyzed against water prior to analysis. Each protein solution (100 μM) was picked up with Litholoop (ϕ = 0.3 mm) and then was flash-frozen under a cryo-nitrogen stream at 100 K. The frozen samples were shipped to SPring-8 BL26B2 for mail-in data collection [13]. The fluorescence XAFS spectra of these proteins were measured automatically by the SPring-8 Precise Automatic Cryo-sample Exchanger (SPACE) [14,15] in the energy range from 1.290000 to 1.276000 Å with an interval of 0.0001 Å for an exposure time of 3 s with a Si-PIN photodiode detector [16]. The XAFS spectra were analyzed using the software D-Cha (database for crystallography with home-lab arrangement) [13] to assign the wavelengths corresponding to the peak and edge.

2.4. Analysis of LECT2 oligomerization in vitro

Twenty microliters of reaction buffer C (100 mM Tris–HCl pH 7.5, 150 mM NaCl) containing recombinant mouse LECT2 (1 μg) were incubated at 37 °C. To assess the role of divalent ions, we included 5 mM of each reagent (EDTA, EGTA, $ZnCl_2$, $MgCl_2$, $CaCl_2$) in the reaction solution. The reaction was stopped by adding an equal volume of SDS–PAGE sample buffer (250 mM Tris–HCl pH 6.8, 10% lithium dodecyl sulfate, 20% glycerol, 0.04% bromophenol blue) and incubating for 1 h at room temperature. The protein samples (2–8 μl) were subjected to SDS–PAGE on a 5–20% gradient polyacrylamide gel and Western blotting using an anti-mouse LECT2 polyclonal antibody [12]. To examine the reversibility of the zinc ion binding to LECT2, we prepared an EDTA-free solution and two EDTA-containing solutions. Forty microliters of buffer C containing 2 μg of recombinant mouse LECT2 were incubated in the presence or absence of 5 mM EDTA for 6 h at 4 °C. Subsequently, the ETDA-free solution was dialyzed using an Xpress micro Dialyze Cartridge 3.5 kDa (Scienova GmbH, Jena, Germany) against 2 ml of buffer C for 12 h as a control. Each of the EDTA-containing solutions was dialyzed using the same cartridge against buffer C (2 ml) with or without 5 mM $ZnCl_2$ for 12 h at 4 °C. The three dialyzed solutions were then separately re-dialyzed three times against 2 ml of buffer C for 12 h at 4 °C. Finally, these solutions were incubated for 24 h at 37 °C and were subjected to SDS–PAGE and Western blot analysis. All SDS–PAGE were carried out under non-reducing conditions (without DTT treatment and boiling) except when indicated specifically.

3. Results

3.1. Recombinant mammalian LECT2 contains a zinc atom

LECT2 is a member of the peptidase M23 structural family (PF01551 in the pfam data base), indicating it is a metalloprotease containing a zinc ion as a cofactor. Therefore, we first attempted to determine whether LECT2 contains a zinc atom. EMI-MS is an appropriate technique with which to analyze peptide–metal interactions [17]. We used the same preparation of the recombinant mouse LECT2 that was analyzed previously using matrix-assisted laser desorption/ionization time-of-flight mass spectrometry [3], which had indicated the only covalent modification was the presence of three disulfide bonds. Fig. 1 shows typical ESI-MS spectra of the recombinant mouse LECT2 under acidic and neutral conditions. The deconvoluted results from analyzing the raw data (Fig. 1A and B) are shown in Fig. 1C and D, respectively. A mass spectrum of the protein under denaturing acidic conditions showed only one predominant peak having a molecular mass of 14633 Da, which was almost identical to the theoretical molecular mass of mature LECT2 [2]. On the other hand, the spectrum of the protein under neutral conditions showed a significant signal of 14698 Da in addition to a major signal of 14633 Da that corresponded to the molecular weight revealed under acidic conditions. The mass difference of these two signals is 65 Da, which is almost identical to the atomic weight of zinc.

To confirm that the zinc atom is bound to LECT2, XAFS measurements were performed. Typical profiles of XAFS experiments are shown in Fig. 2. The XAFS profile of recombinant mouse LECT2 in Fig. 2A showed a *K* absorption edge of 1.2828 Å, indicating the protein contained a zinc atom [18]. A positive control experiment using the zinc-binding protein lysostaphin [19,20] is shown in Fig. 2B. The *K* absorption edge (1.2828 Å) wavelength indicating zinc absorption in lysostaphin was identical to that seen in the LECT2 XAFS data. These data indicate that recombinant mouse LECT2 contains a non-covalently bound zinc atom and strongly suggest that there is one zinc atom per molecule.

3.2. Oligomerization of mammalian LECT2 in vitro

The incubation experiments revealed that recombinant mammalian LECT2s oligomerize in vitro. Recombinant mouse LECT2

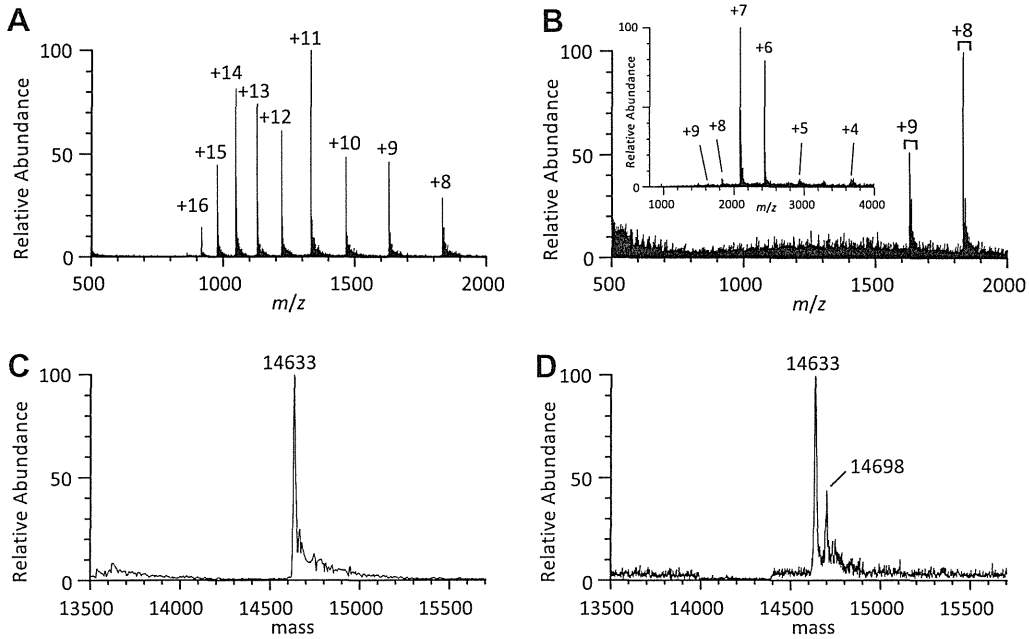

Fig. 1. *Comparisons of electrospray ionization (ESI) mass spectra of mouse LECT2 under acidic (0.075% formic acid) and neutral (10 mM ammonium formate) conditions.* Positive ion ESI mass spectra of LECT2 under acidic (A) and neutral (B) conditions. Charge states of LECT2 protein ions are indicated. The corresponding deconvoluted spectra of LECT2 under acidic (C) and neutral (D) conditions. The wider *m/z* range mass spectrum insets are shown in the upper left corner of the neutral conditions figure (B). Calculated molecular weights are indicated.

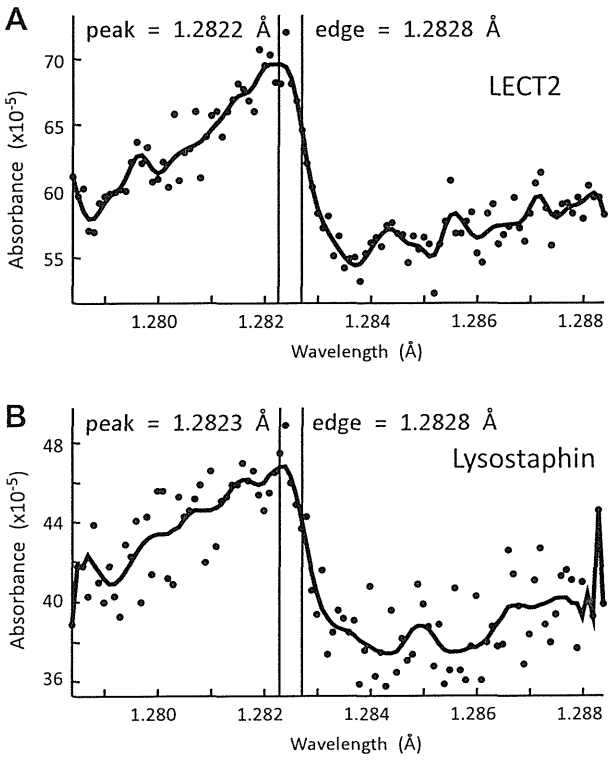

Fig. 2. A comparison of the fluorescence XAFS data at the Zn *K* absorption edge of LECT2 (A) and lysostaphin (B).

was incubated in buffer C (100 mM Tris–HCl pH 7.5, 150 mM NaCl) at 37 °C for one day. SDS–PAGE was then performed under non-reducing conditions, and LECT2 protein was detected by Western blotting using an anti-mouse LECT2 polyclonal antibody. Fig. 3A shows that the oligomerization occurred in a temperature-dependent manner. As shown in Supplemental Fig. 1, the oligomerization occurred in a time-dependent manner. SDS–PAGE carried out under reducing conditions showed a distinct pattern of oligomerization. Strangely, ladder bands migrating at 100–250 kDa and smear bands around the expected dimer position were detected in reduced SDS–PAGE. As shown in Supplemental Fig. 2, DTT treatment enhanced the oligomerization of LECT2 in a concentration-dependent manner. Furthermore, the intensity of the ladder bands migrating between 100 and 250 kDa increased over time in the experiments carried out at the high concentration of 200 mM DTT (Supplemental Fig. 3). Moreover, the state of the dimer in reduced SDS–PAGE was different from those observed in non-reduced SDS–PAGE. On the other hand, iodoacetate is known to be an alkylating agent, which irreversibly reacts with cysteine to block disulfide bond formation. As shown in Supplemental Fig. 4, iodoacetate treatment inhibited higher-order oligomerization except dimers and trimers. Strangely, the formation of lower-order oligomers increased at 10 mM of iodoacetate. The mechanism behind these oligomerization variations is not clear, but the disulfide bonds among LECT2s appeared to be involved in oligomer formation. As shown in Fig. 3A, oligomers of LECT2 were not detectable on a silver-stained gel following a 1-day incubation.

Oligomerization of recombinant human LECT2 produced by an animal cell line has also been observed, indicating that the oligomerization was not unique to mouse LECT2 (Fig. 3B).

3.3. Zinc suppresses oligomerization of mammalian LECT2

As shown in Fig. 4A, treatment with EDTA as a zinc ion chelator enhanced the oligomerization of LECT2, and Zn^{2+} reduced it as compared with an untreated control (lanes 2 and 4 vs. lane 1). EGTA treatment also enhanced the oligomerization of LECT2 to a similar extent (lane 3). Both Ca^{2+} and Mg^{2+} ions slightly inhibited the oligomerization (lanes 5 and 6), but that inhibition was much lower than that seen following Zn^{2+} treatment. Furthermore, the possibility that incorporation of the zinc ion was reversible in LECT2 was explored. As shown in Fig. 4B, LECT2 was treated with EDTA for 6 h, and then EDTA was removed by dialysis against

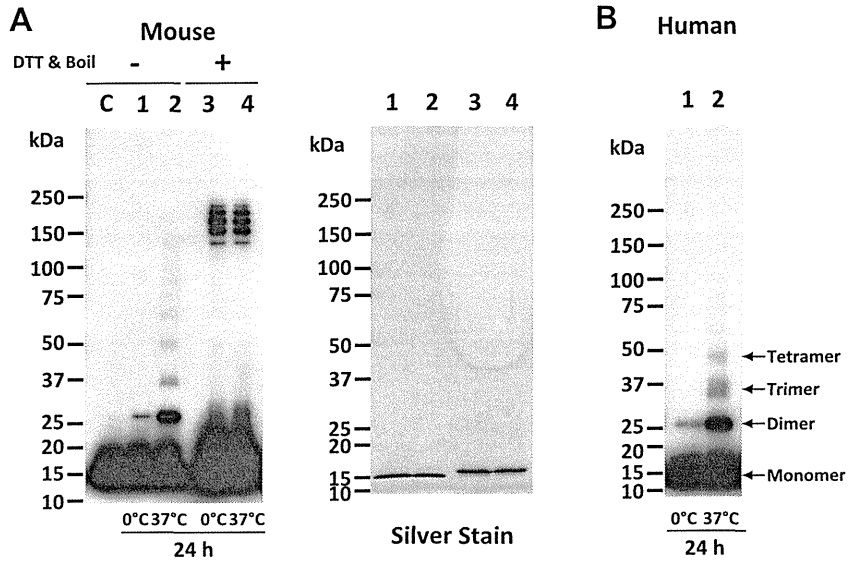

Fig. 3. Oligomerization assay of LECT2 in vitro. (A) Reaction solutions containing recombinant mouse LECT2 were incubated for 24 h at 0 °C (lanes 1 and 3) and 37 °C (lanes 2 and 4). Each reaction was divided into two aliquots, and the reactions were stopped by adding SDS–PAGE sample buffer without (lanes 1 and 2) or with (lanes 3 and 4) DTT (200 mM) and boiling (for 5 min). SDS–PAGE was then carried out on a 5–20% gradient polyacrylamide gel followed by Western blotting. A non-incubated sample was loaded in the first lane (C). Left image: Western blot. Right image: silver stained gel. (B) Recombinant human LECT2 was incubated for 24 h at 0 °C (lane 2) and 37 °C (lane 3).

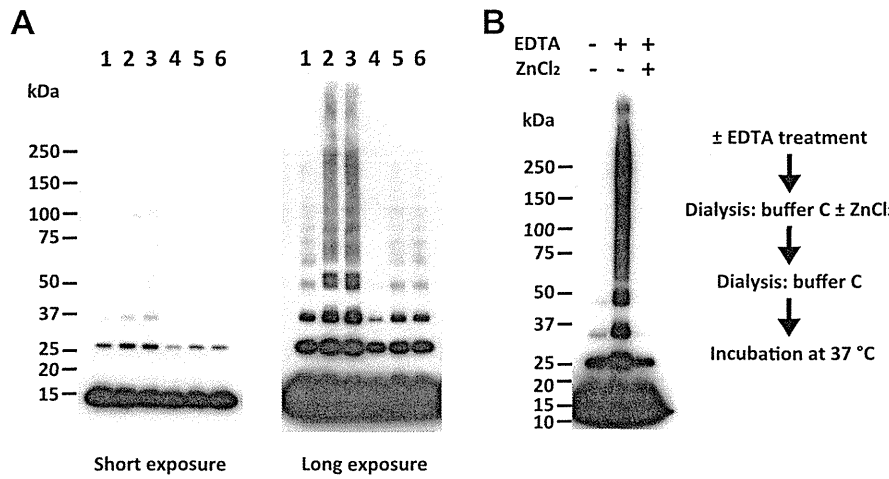

Fig. 4. *Zinc inhibits the oligomerization of LECT2 in vitro.* (A) *The recombinant mouse LECT2 protein solution was incubated with chelators or divalent cations for* 24 h 37 °C and then analyzed by SDS–PAGE and Western blotting. Lane: 1, control; 2, 5 mM EDTA; 3, 5 mM EGTA; 4, 5 mM $ZnCl_2$; 5, 5 mM $CaCl_2$; 6, 5 mM $MgCl_2$. Left image: short exposure of Western blot. Right image: long exposure of Western blot. (B) The effect of added zinc on EDTA-treated LECT2. Two aliquots of recombinant mouse LECT2 protein solution were incubated with 5 mM EDTA for 6 h at 4 °C and then dialyzed against buffer C (lane 2) or buffer C containing 5 mM $ZnCl_2$ and subsequently against buffer C to remove excess zinc ions (lane 3). In parallel, an aliquot of LECT2 solution as a control was incubated without EDTA for 6 h at 4 °C and then dialyzed against buffer C (lane 1). All dialyses were carried out at 4 °C. Following the final dialysis against fresh buffer C, all three samples were incubated for 24 h at 37 °C and then analyzed by SDS–PAGE and Western blotting.

buffer C with or without 5 mM $ZnCl_2$. Free zinc ions were subsequently removed by dialysis against buffer C. Consequently, oligomerization stimulated by EDTA treatment was suppressed to below the control level by introduction of zinc. Taken together, these results indicated that zinc contributed to the stabilization of the LECT2 structure and strongly suggested that incorporation of the zinc ion in LECT2 was reversible.

4. Discussion

Zinc is known to play a structural or catalytic role in many proteins [21]. The sequence homology of LECT2 with a zinc metalloprotease family suggested that zinc might stabilize the LECT2 structure. The effect of zinc on the oligomerization state of LECT2 was therefore examined. This report presents the results of ESI-MS and XAFS analyses, which demonstrate that LECT2 contains a non-covalently bound zinc atom. LECT2 is a member of the peptidase M23 family. The structures of four proteins in this family have been determined by X-ray crystallography (PDBj; http://www.pdbj.org). Three additional members of the M23B subfamily were identified by a homology search with LECT2, which contains two conserved motifs (HxxD and HxH) that were associated with zinc ion binding in these three proteins. Fig. 5 shows the corresponding amino acid sequence alignments. Each member of this family has one zinc ion per protein molecule. Together with ESI-MS data presented herein, this indicates that mammalian LECT2 also binds to one zinc ion per molecule.

Our results also demonstrate that mammalian LECT2 protein oligomerizes in vitro. Mammalian LECT2 has three disulfide bonds [3]. The oligomerization was strongly affected by DTT treatment, as

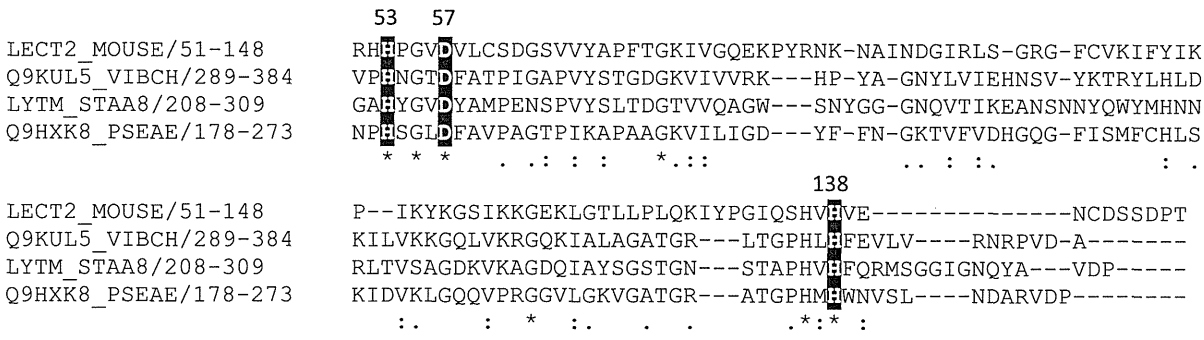

Fig. 5. Alignments of the zinc binding regions of mouse LECT2 and other peptidase M23B family proteins. Q9KUL5_VIBCH; Putative uncharacterized protein VC0503 from *Vibrio cholerae*, LYTM_STAA8; Glycyl-glycine endopeptidase LytM from *Staphylococcus aureus* strain NCTC 8325, Q9HXK8_PSEAE; Putative uncharacterized protein from *Pseudomonas aeruginosa*. Putative amino acid residues that directly bind to zinc are shown in black boxes.

shown in Fig. 3B and in Supplemental Figs. 2 and 3. Furthermore, the inhibition of higher-order oligomer formation by iodoacetate treatment as shown in Supplemental Fig. 4 also reflects the contribution of disulfide bonds. Dimer (occasionally trimer and tetramer) formation was found at low temperature and in the presence of zinc or iodoacetate. The kinetics of lower-order oligomer formation might be faster than that of higher-order oligomer formation. LECT2 might non-covalently form oligomers under physiological conditions. Actually, Mim-1, which is the chicken ortholog of LECT2, consists of two repeated units of LECT2 that associate to form a dimer [22]. Oligomers of LECT2 were not detectable on a silver-stained gel following a 1-day incubation (Fig. 3B). A faint band at the assumed positions for dimers was detected following a 7-day incubation, but further oligomerization of LECT2 over that incubation period was not observed (data not shown). Considering the sensitivity of the silver-stain, we estimate one or less percent of total LECT2 was involved in this reaction. The most likely explanation for this low reactivity is that the most of the cysteine residues in the recombinant LECT2 formed sulfide bonds. Therefore only a small number of residual cysteine residues that did not form the disulfide bonds were available to participate in this reaction. It is known that oligomerization of a recombinant protein is occasionally caused by oxidation [23,24]. On the other hand, it is possible that another structural property of LECT2 caused the oligomerization, as in the case of β_2-microglobulin [25].

LECT2 contains a zinc atom, and zinc ions inhibited the formation of oligomers, indicating that zinc stabilizes the LECT2 structure. ESI-MS analysis has also been used to monitor protein folding and protein complexes [26]. In comparing Fig. 1A and B, it appears that fewer accessible protonation sites would partially reflect a more compact LECT2 protein folding induced by zinc complex formation. It is possible that zinc plays a crucial role in LECT2 activity as well. For example, as LECT2 is a member of the M23 protease family, we are analyzing the possibility that it is a protease. Until now, we have not found any protease activities of LECT2 after testing it against many possible protein substrates (serum albumin, carbonic anhydrase, insulin-beta chain, aprotinin and ribonuclease A in bovine, rabbit myosin and phosphorylase b, hen egg ovalbumin and lysozyme, soybean trypsin inhibitor, glutathione S-transferase of *Schistosoma japonicum*, maltose binding protein and β-galactosidase of *Escherichia coli*; data not shown). Furthermore, we could not find any lysostaphin-like activity of LECT2 against *Staphylococcus aureus* (data not shown) [27]. If LECT2 has a protease activity, the substrate specificity might be strict. On the other hand, LECT2 might not have a protease activity similar to murein hydrolase activator NlpD protein, which also belongs to the M23 protease family [28].

Recently, it has been reported that LECT2 is a novel renal amyloid protein [10]. Although LECT2 amyloidosis has been recognized only recently, it does not appear to be a rare occurrence [11]. One feature of amyloid proteins is their beta-sheet rich structures. Actually, some amyloid proteins, such as immunoglobulin light chain, β_2-microglobulin and lysozyme, have extensive beta-sheet structure in their native state, and a beta-sheet may be stabilized by protein aggregation [29]. We have already indicated that LECT2 has several beta-sheets but no alpha-helix [30]. The oligomerization of LECT2 might offer a clue for further investigations of amyloid fibril formation, to further clarify the mechanism of LECT2 oligomerization.

Acknowledgments

We thank Drs. Yuuki Nakamura, Go Ueno, Takaaki Hikima and Masaki Yamamoto for help with XAFS analysis using the mail-in system in SPring-8. We also thank Akio Ebihara, Mayumi Kanagawa and Yoshiaki Kitamura for their help in data collection at the SPring-8 beamlines BL26B1 and BL26B2. Finally, we thank Drs. Koichi Tanabe and Keiko Ishino for useful discussions. This work was supported in part by Grants-in-Aid for Scientific Research from the Ministry of Education, Science, Sports and Technology of Japan (MEXT) to A. Okumura (21791422 and 24790938) and S. Yamagoe (23590275), and by the X-ray Free Electron Laser Utilization Research Project of MEXT to N. Dohmae.

Appendix A. Supplementary data

Supplementary data associated with this article can be found, in the online version, at http://dx.doi.org/10.1016/j.febslet.2013.01.025.

References

[1] Yamagoe, S., Yamakawa, Y., Matsuo, Y., Minowada, J., Mizuno, S. and Suzuki, K. (1996) Purification and primary amino acid sequence of a novel neutrophil chemotactic factor LECT2. Immunol. Lett. 52, 9–13.
[2] Yamagoe, S., Mizuno, S. and Suzuki, K. (1998) Molecular cloning of human and bovine LECT2 having a neutrophil chemotactic activity and its specific expression in the liver. Biochim. Biophys. Acta 1396, 105–113.
[3] Okumura, A., Suzuki, T., Dohmae, N., Okabe, T., Hashimoto, Y., Nakazato, K., Ohno, H., Miyazaki, Y. and Yamagoe, S. (2009) Identification and assignment of three disulfide bonds in mammalian leukocyte cell-derived chemotaxin 2 by matrix-assisted laser desorption/ionization time-of-flight mass spectrometry. Biosci. Trends 3, 139–143.
[4] Saito, T., Okumura, A., Watanabe, H., Asano, M., Ishida-Okawara, A., Sakagami, J., Sudo, K., Hatano-Yokoe, Y., Bezbradica, J.S., Joyce, S., Abo, T., Iwakura, Y., Suzuki, K. and Yamagoe, S. (2004) Increase in hepatic NKT cells in leukocyte cell-derived chemotaxin 2-deficient mice contributes to severe concanavalin A-induced hepatitis. J. Immunol. 173, 579–585.
[5] Okumua, A., Saito, T., Otani, I., Kojima, K., Yamada, Y., Ishida-Okawara, A., Nakazato, K., Asano, M., Kanayama, K., Iwakura, Y., Suzuki, K. and Yamagoe, S. (2008) Suppressive role of leukocyte cell-derived chemotaxin 2 in mouse antitype II collagen antibody-induced arthritis. Arthritis Rheum. 58, 413–421.
[6] Phesse, T.J., Parry, L., Reed, K.R., Ewan, K.B., Dale, T.C., Sansom, O.J. and Clarke, A.R. (2008) Deficiency of Mbd2 attenuates Wnt signaling. Mol. Cell. Biol. 28, 6094–6103.

[7] Dang, M.H., Kato, H., Ueshiba, H., Omori-Miyake, M., Yamagoe, S., Ando, K., Imanishi, K., Arimura, Y., Haruta, I., Kotani, T., Ozaki, M., Suzuki, K., Uchiyama, T. and Yagi, J. (2010) Possible role of LECT2 as an intrinsic regulatory factor in SEA-induced toxicity in D-galactosamine-sensitized mice. Clin. Immunol. 137, 311–321.
[8] Ong, H.T., Tan, P.K., Wang, S.M., Hian Low, D.T., Ooi, L.L. and Hui, K.M. (2011) The tumor suppressor function of *LECT2* in human hepatocellular carcinoma makes it a potential therapeutic target. Cancer Gene Ther. 18, 399–406.
[9] Anson, M., Crain-Denoyelle, A.M., Baud, V., Chereau, F., Gougelet, A., Terris, B., Yamagoe, S., Colnot, S., Viguier, M., Perret, C. and Couty, J.P. (2012) Oncogenic β-catenin triggers an inflammatory response that determines the aggressiveness of hepatocellular carcinoma in mice. J. Clin. Invest. 122, 586–599.
[10] Benson, M.D., James, S., Scott, K., Liepnieks, J.J. and Kluve-Beckerman, B. (2008) Leukocyte chemotactic factor 2: a novel renal amyloid protein. Kidney Int. 74, 218–222.
[11] Murphy, C.L., Wang, S., Kestler, D., Larsen, C., Benson, D., Weiss, D.T. and Solomon, A. (2010) Leukocyte chemotactic factor 2 (LECT2)-associated renal amyloidosis: a case series. Am. J. Kidney Dis. 56, 1100–1107.
[12] Yamagoe, S., Akasaka, T., Uchida, T., Hachiya, T., Okabe, T., Yamakawa, Y., Arai, T., Mizuno, S. and Suzuki, K. (1997) Expression of a neutrophil chemotactic protein LECT2 in human hepatocytes revealed by immunochemical studies using polyclonal and monoclonal antibodies to a recombinant LECT2. Biochem. Biophys. Res. Commun. 237, 116–120.
[13] Okazaki, N., Hasegawa, K., Ueno, G., Murakami, H., Kumasaka, T. and Yamamoto, M. (2008) Mail-in data collection at SPring-8 protein crystallography beamlines. J. Synchrotron Radiat. 15, 288–291.
[14] Ueno, G., Hirose, R., Ida, K., Kumasaka, T. and Yamamoto, M. (2004) Sample management system for a vast amount of frozen crystals at SPring-8. J. Appl. Crystallogr. 37, 867–873.
[15] Ueno, G., Kanda, H., Kumasaka, T. and Yamamoto, M. (2005) Beamline Scheduling Software: administration software for automatic operation of the RIKEN structural genomics beamlines at SPring-8. J. Synchrotron Radiat. 12, 380–384.
[16] Ueno, G., Kanda, H., Hirose, R., Ida, K., Kumasaka, T. and Yamamoto, M. (2006) RIKEN structural genomics beamlines at the SPring-8; high throughput protein crystallography with automated beamline operation. J. Struct. Funct. Genomics 7, 15–22.
[17] Loo, J.A. (1997) Studying noncovalent protein complexes by electrospray ionization mass spectrometry. Mass Spectrom. Rev. 16, 1–23.
[18] Sasaki, S. (1989) Numerical tables of anomalous scattering factors calculated by the Cromer and Liberman's method. KEK Report 14–88, 1–136.
[19] Trayer, H.R. and Buckley III, C.E. (1970) Molecular properties of lysostaphin, a bacteriolytic agent specific for *Staphylococcus aureus*. J. Biol. Chem. 245, 4842–4846.
[20] Odintsov, S.G., Sabala, I., Marcyjaniak, M. and Bochtler, M. (2004) Latent LytM at 1.3 Å resolution. J. Mol. Biol. 335, 775–785.
[21] Lee, Y.M. and Lim, C. (2008) Physical basis of structural and catalytic Zn-binding sites in proteins. J. Mol. Biol. 379, 545–553.
[22] Ness, S.A., Marknell, A. and Graf, T. (1989) The *v-myb* oncogene product binds to and activates the promyelocyte-specific *mim-1* gene. Cell 59, 1115–1125.
[23] Yamamoto, Y., Kato, Z., Matsukuma, E., Li, A., Omoya, K., Hashimoto, K., Ohnishi, H. and Kondo, N. (2004) Generation of highly stable IL-18 based on a ligand–receptor complex structure. Biochem. Biophys. Res. Commun. 317, 181–186.
[24] Seno, M., Sasada, R., Iwane, M., Sudo, K., Kurokawa, T., Ito, K. and Igarashi, K. (1988) Stabilizing basic fibroblast growth factor using protein engineering. Biochem. Biophys. Res. Commun. 151, 701–708.
[25] Liu, C., Sawaya, M.R. and Eisenberg, D. (2011) β_2-microglobulin forms three-dimensional domain-swapped amyloid fibrils with disulfide linkages. Nat. Struct. Mol. Biol. 18, 49–55.
[26] Winston, R.L. and Fitzgerald, M.C. (1997) Mass spectrometry as a readout of protein structure and function. Mass Spectrom. Rev. 16, 165–179.
[27] DeHart, H.P., Heath, H.E., Heath, L.S., LeBlanc, P.A. and Sloan, G.L. (1995) The lysostaphin endopeptidase resistance gene (*epr*) specifies modification of peptidoglycan cross bridges in *Staphylococcus simulans* and *Staphylococcus aureus*. Appl. Environ. Microbiol. 61, 1475–1479.
[28] Uehara, T., Parzych, K.R., Dinh, T. and Bernhardt, T.G. (2010) Daughter cell separation is controlled by cytokinetic ring-activated cell wall hydrolysis. EMBO J. 29, 1412–1422.
[29] Soto, C. (2001) Protein misfolding and disease; protein refolding and therapy. FEBS Lett. 498, 204–207.
[30] Ito, M., Nagata, K., Yumoto, F., Yamagoe, S., Suzuki, K., Adachi, K. and Tanokura, M. (2004) ^{1}H, ^{13}C, ^{15}N resonance assignments of the cytokine LECT2. J. Biomol. NMR 29, 543–544.